Electronic Supplementary Material (ESI) for Dalton Transactions.

Supplementary Information

Tin Guanidinato Complexes: Oxidative Control of Sn, SnS, SnSe and SnTe Thin Film Deposition

I. Y. Ahmet,[a] M.S.Hill*[a,b], P.R. Raithby[b] and A. L. Johnson*[a,b]

[a] *Centre for Sustainable Chemical Technologies*
Department of Chemistry,
University of Bath. Claverton Down, Bath, BA2 7AY, UK.

[b] *Department of Chemistry,*
University of Bath. Claverton Down, Bath, BA2 7AY, UK
E-mail: M.S.Hill@Bath.ac.uk & A.L.Johnson@bath.ac.uk

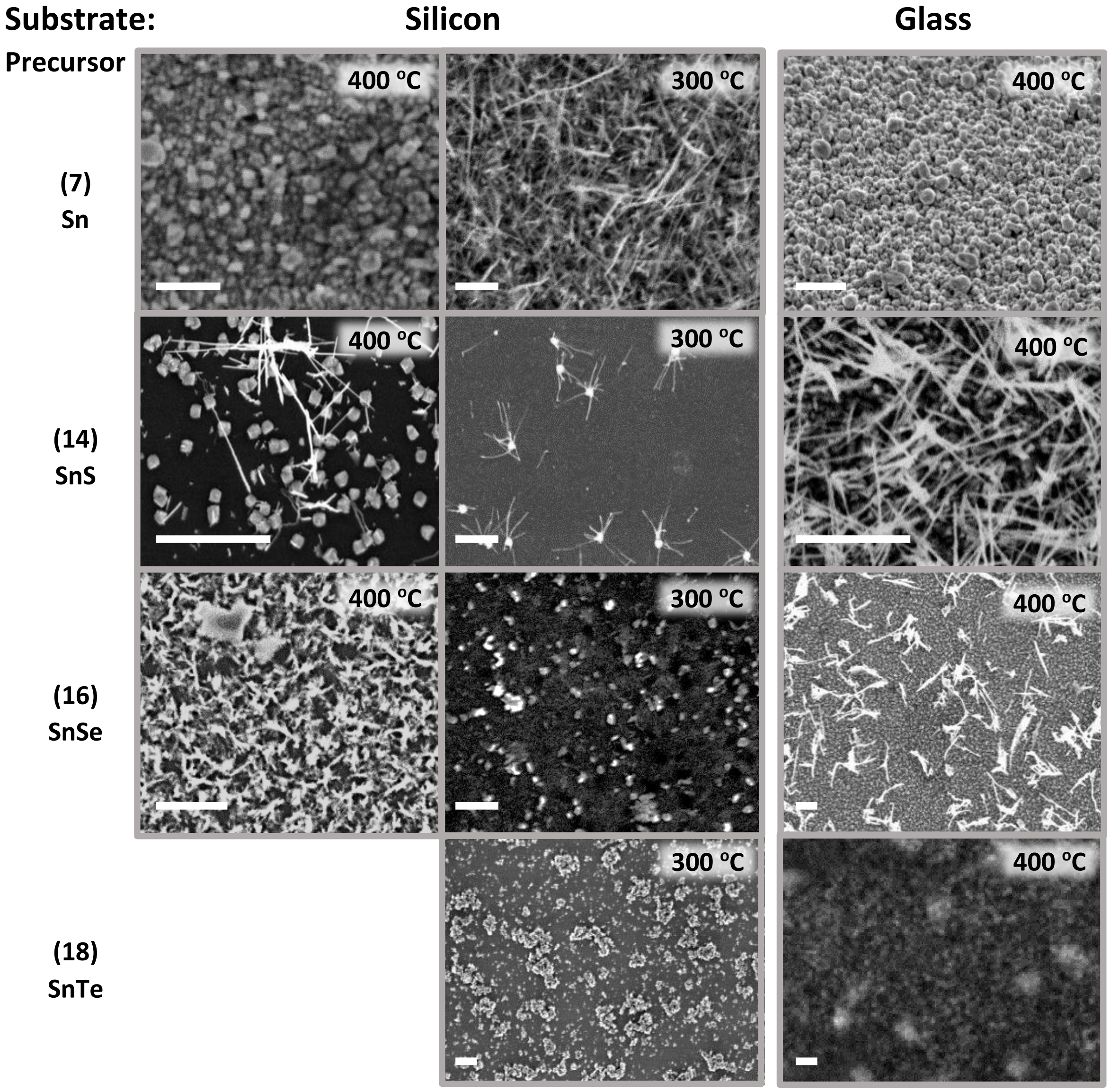

Figure S1: SEM images of AA-CVD deposited Thin Films onto c-Si at 300 and 400 ^{o}C and at 400 $_{o}$C onto glass, from precursors **7**, **14**, **16** and **18** (0.033M solutions).

Table S1: EDS analysis of AA-CVD deposited Thin Films onto c-Si at 400 ^{o}C from precursors **7**, **14**, **16** and **18** (0.033M Solution).

	Atomic %			
Precursor	**Sn**	**Ch**	**C**	**O**
7 (Sn)	97.35	-	-	2.65
14 (SnS)*	20.54	15.87	10.11	9.87
16 (SnSe)*	3. 92	3.12	4.53	1.52
18 (SnTe)*	1.21	1.51	6.72	2.89

*: The thin films deposited have a low degree of coverage, which are consistent with EDS analysis which shows a high Si% (SnS: 43.61%, SnSe: 86.91%, SnTe: 87.67%) from the underlying substrate.

Figure S2: PXRD pattern for Sn deposited onto glass at 400^{o}C from precursor **7** using a 0.033M precursor concentrations.

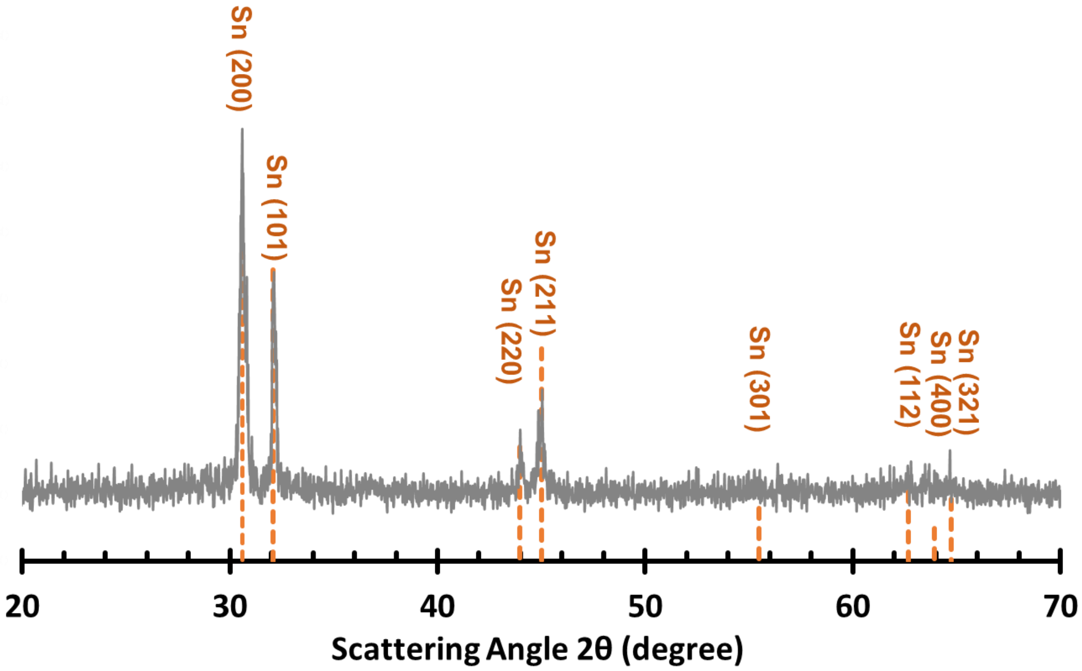

Figure S3: PXRD pattern for α-SnS films deposited onto glass at 400^{o}C from precursor **14** using a a 0.033M toluene precursor solution.

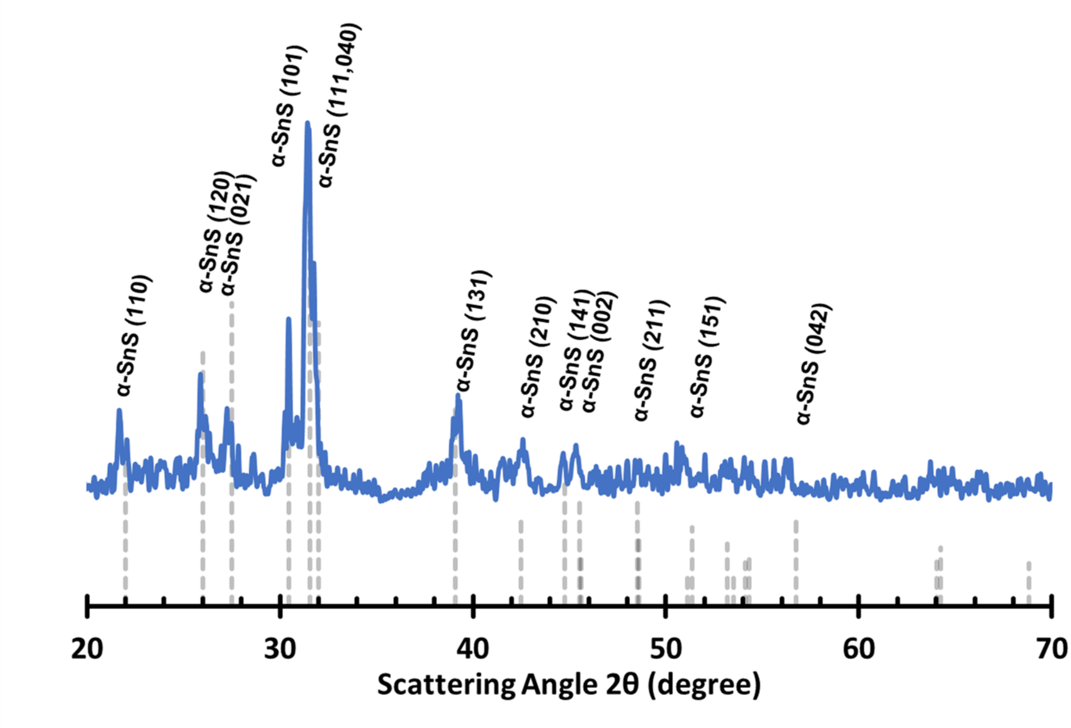

Figure S4: Stacked PXRD patterns for deposited films of α-SnSe, deposited onto c-Si at (a) 300 ^{o}C and (b) 400 ^{o}C, and onto (c) glass at 400 ^{o}C from precursor **16** using a 0.033M toluene precursor solution.

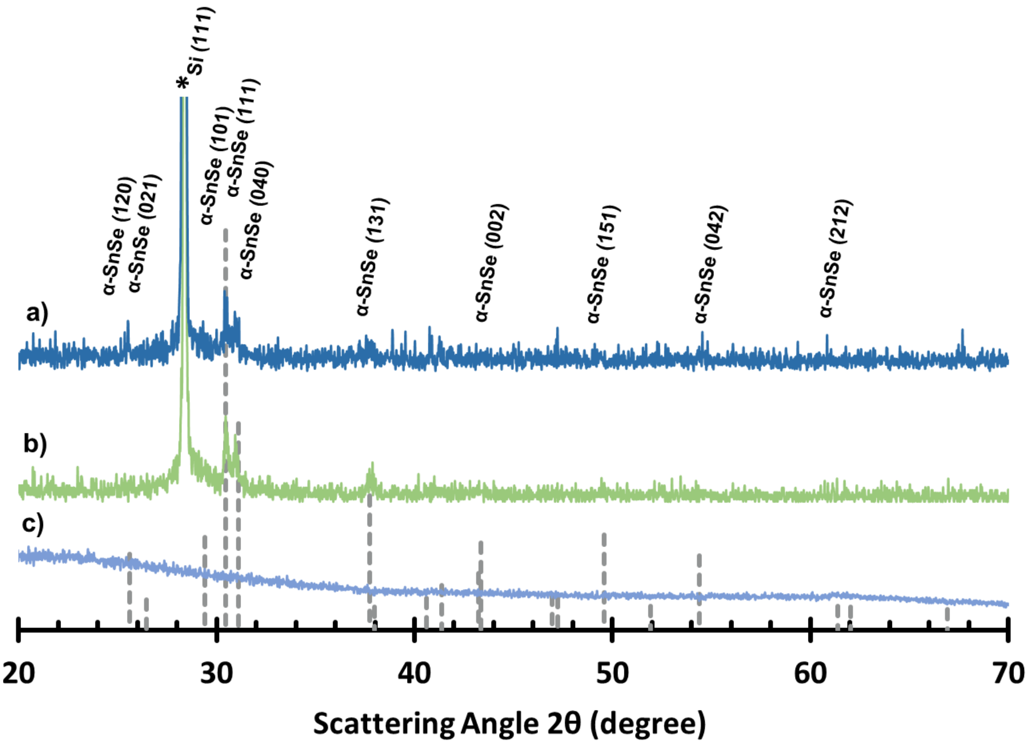

Figure S5: Stacked PXRD patterns for deposited films of SnTe, deposited onto c-Si at (a) 300 °C and (b) 400 °C, and onto (c) glass at 400 °C from precursor **18** using a 0.033M toluene precursor solution.

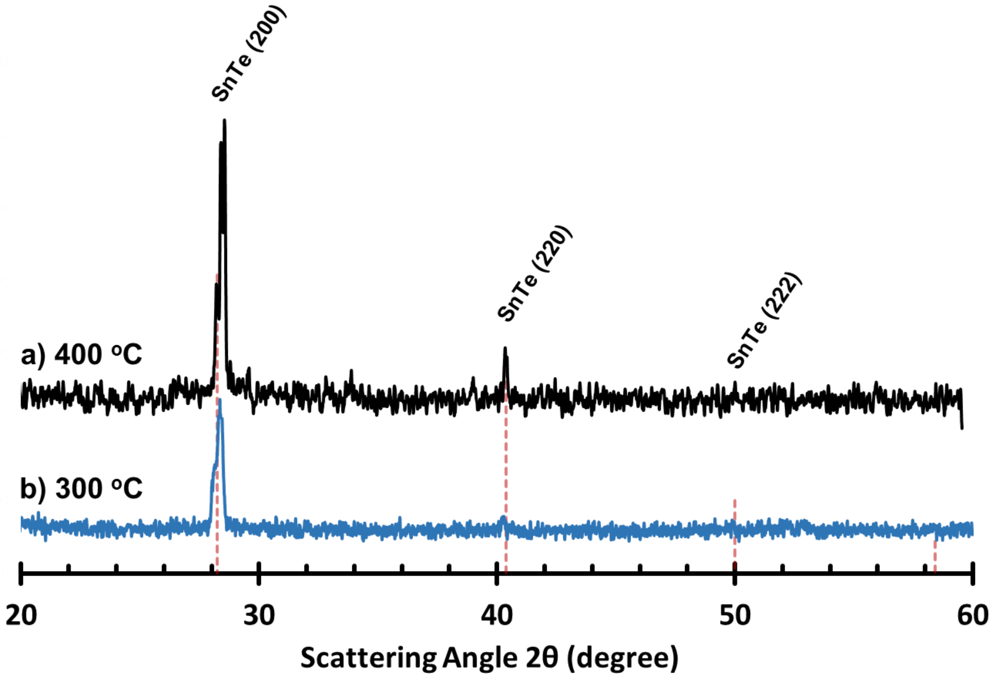

Figure S6: PXRD Pattern of Sn deposited from precursor **6** (0.08M) toluene solution at 400°C onto a glass substrate, this particular sample shows peaks associated with SnO formation after exposure to air for a period of several weeks.

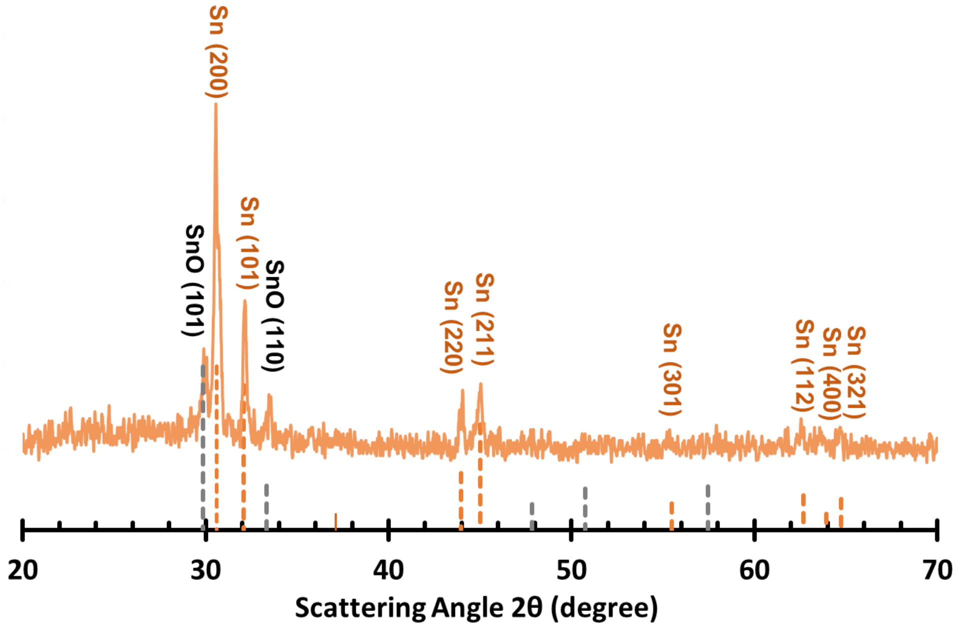

Figure S7: (a) Raman spectrum of the Sn film deposited onto glass from compounds **7** at 300 ^{o}C using an excitation 532 nm laser intensity of 0.1 %. (b) Shows the Raman spectrum of the same region when the laser intensity is increased to 10 %. Increasing the energy of the 532 nm Raman excitation laser resulted in the formation of Raman shifts assigned to SnO and is caused by heating and oxidation of the tin in air. (c) Shows that the SnO peaks persist when the laser intensity is returned to 0.1 %.

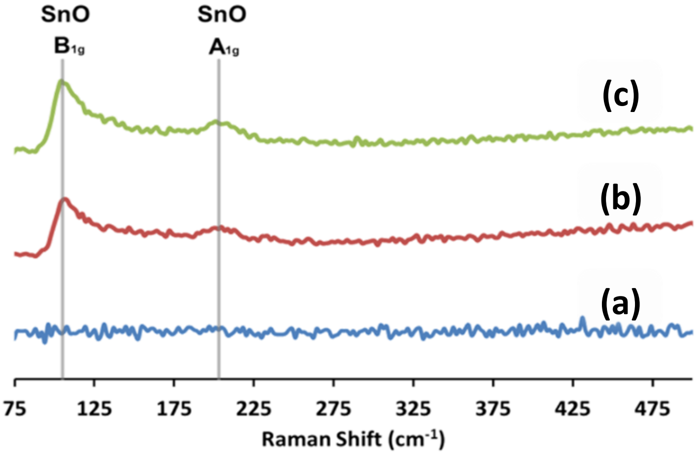

Figure S8: EDS spectra of the Sn films produced by AA-CVD from 0.08M toluene solutions of either (A) **7** onto c-Si or (B) from **6** onto at 400^{oi}C.

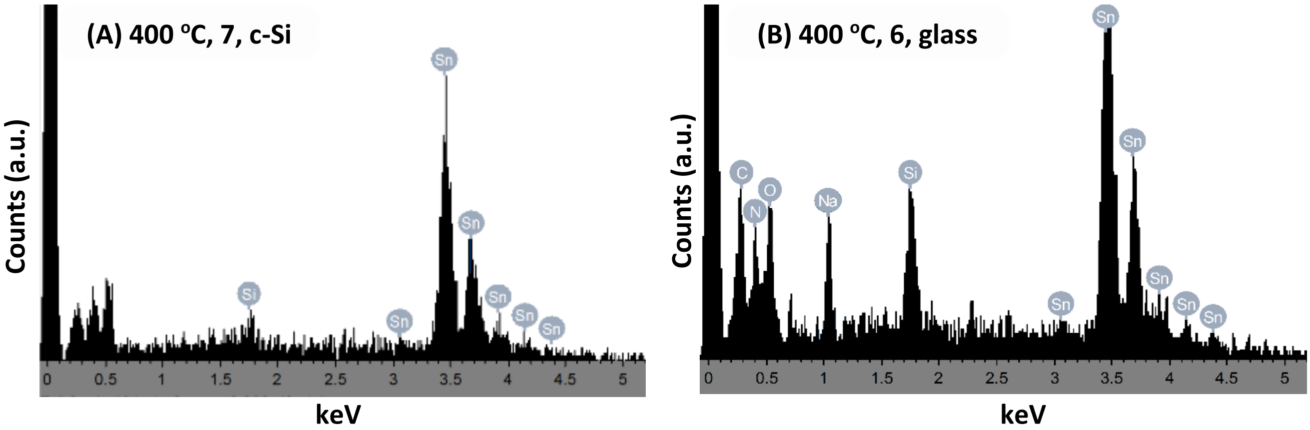

Table S2: EDS analysis of Sn thin films deposited by AA-CVD onto c-Si from **7** and onto glass from **6** at 400^{oi}C, using 0.08M toluene solutions.

	c-Si, Precursor 7			Glass, Precursor 6		
Element	**Wt%**	**At%**	**At%***	**Wt%**	**At%**	**At%***
Si	2.64 ± 0.45	8.84	10.64	8.29 ± 0.36	17.72	30.29
O	3.47 ± 0.97	20.41	-	11.06 ± 0.20	41.51	-
Sn	93.87 ± 0.04	74.21	89.36	80.64 ± 0.44	40.77	69.70

Figure S9: SEM image of the α-SnS AA-CVD film produced from precursor **14** at 300 °C (A) and 400 °C (B) on c-Si substrates, from 0.08M toluene solutions.

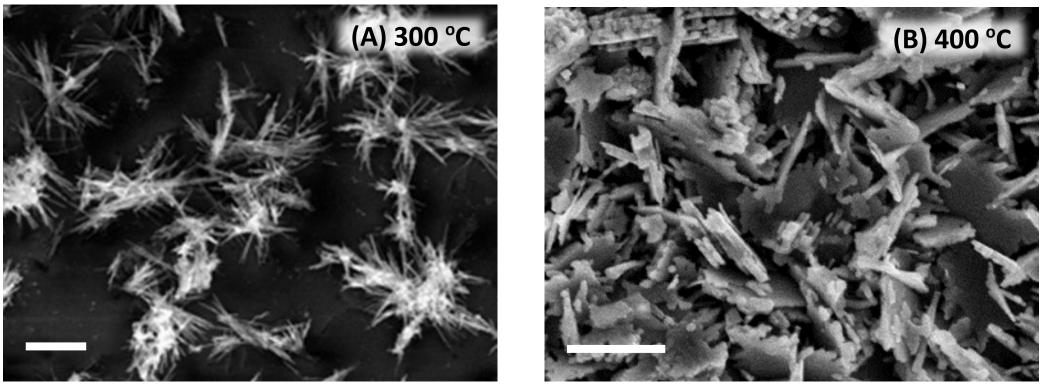

Figure S10: EDS spectra of the α-SnS films produced by AA-CVD from precursor **14** at 300 °C (A) and 400 °C (B) on c-Si substrates, from 0.08M toluene solutions.

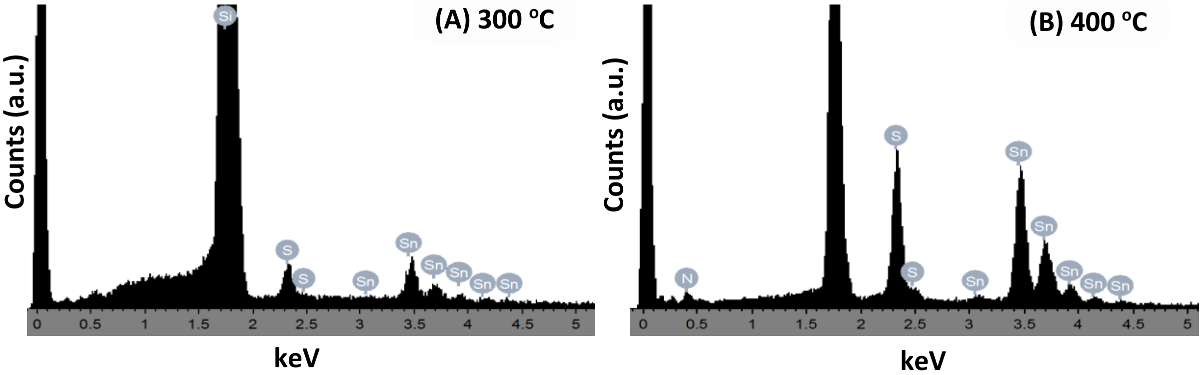

Table S3: EDS analysis of SnSe thin films deposited by AA-CVD onto c-Si at 300^{oi}C and 400 °C from precursor **14** from 0.08M toluene solutions.

	300 °C			400 °C		
Element	**Wt%**	**At%**	**At%***	**Wt%**	**At%**	**At%***
Si	91.85 ± 0.25	96.81	-	69.41 ± 0.28	86.21	-
S	1.71 ± 0.09	1.58	45.66	6.05 ± 0.1	6.58	47.72
Sn	6.44 ± 0.24	1.68	54.94	24.54 ± 0.23	7.21	52.28

Figure S11: PDRX Patterns of α-SnS films obtained at a) 300^{o}C and b) 400 °C on c-Si substrates from the AA-CVD of 0.08M toluene solutions containing complex **14**.

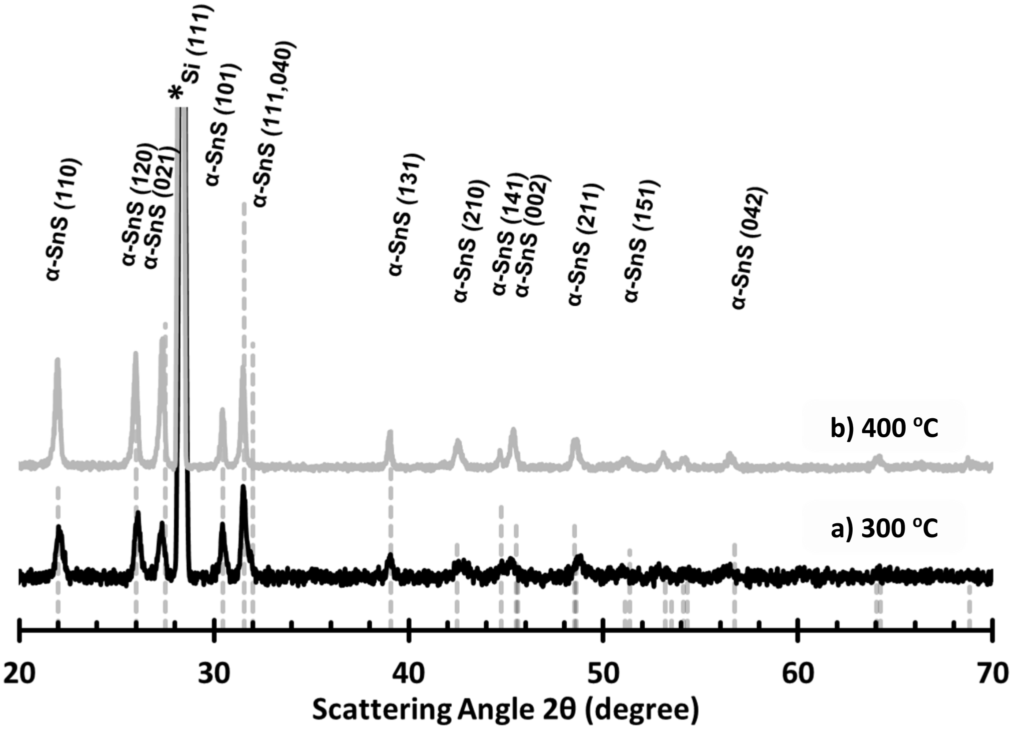

Figure S12: EDS spectra of the AA-CVD α-SnSe films produced from precursor **16** at 400 °C onto (B) c-Si and (B) glass substrates , from 0.08M toluene solutions.

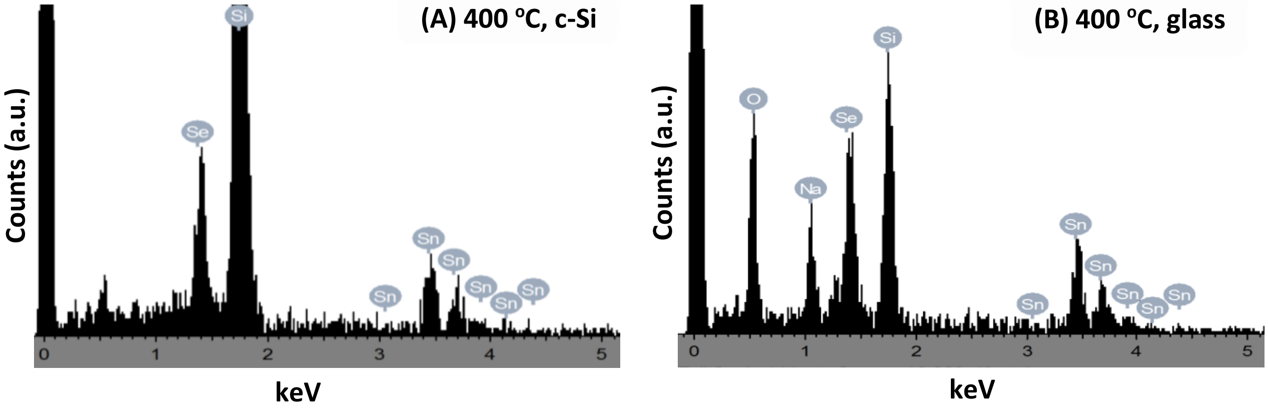

Table S4: EDS analysis of α-SnSe thin films deposited by AA-CVD onto c-Si and Glass substrates at 400 °C from precursors **16** (0.08M Solution).

	c-Silicon			Glass		
Element	**Wt%**	**At%**	**At%***	**Wt%**	**At%**	**At%***
O	-	-	-	30.00 ± 2.07	60.37	-
Na	-	-	-	40.80 ± 0.64	6.72	-
Si	60.46 ± 1.91	80.41	-	14.94 ± 1.04	17.12	-
S	8.40 ± 0.99	9.79	49.96	15.75 ± 1.44	1.44	43.44
Sn	31.14 ± 1.99	9.80	50.04	34.51 ± 2.35	2.35	56.56

Figure S13: AFM micrographs and surface roughness values for Sn thin films deposited by AA-CVD from 0.08 M toluene solutions of precursor **7** at 300 °C onto a glass substrate.

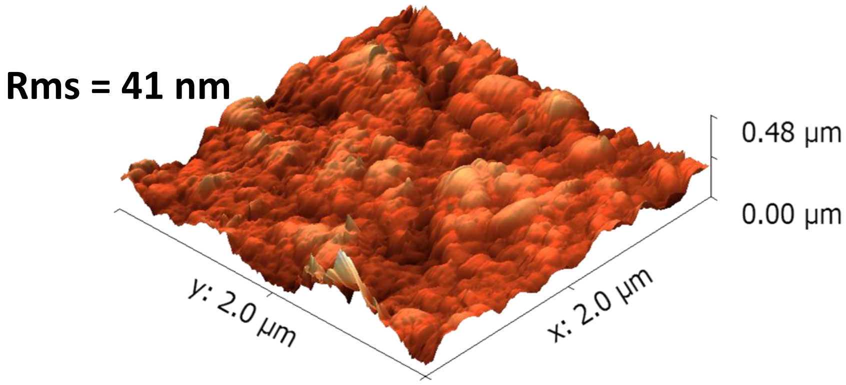

Figure S14: AFM micrographs and surface roughness values for α-SnSe thin films deposited by AA-CVD from 0.08 M toluene solutions of precursor **16** at 400 °C (A) on c-Si and glass (B) substrates.

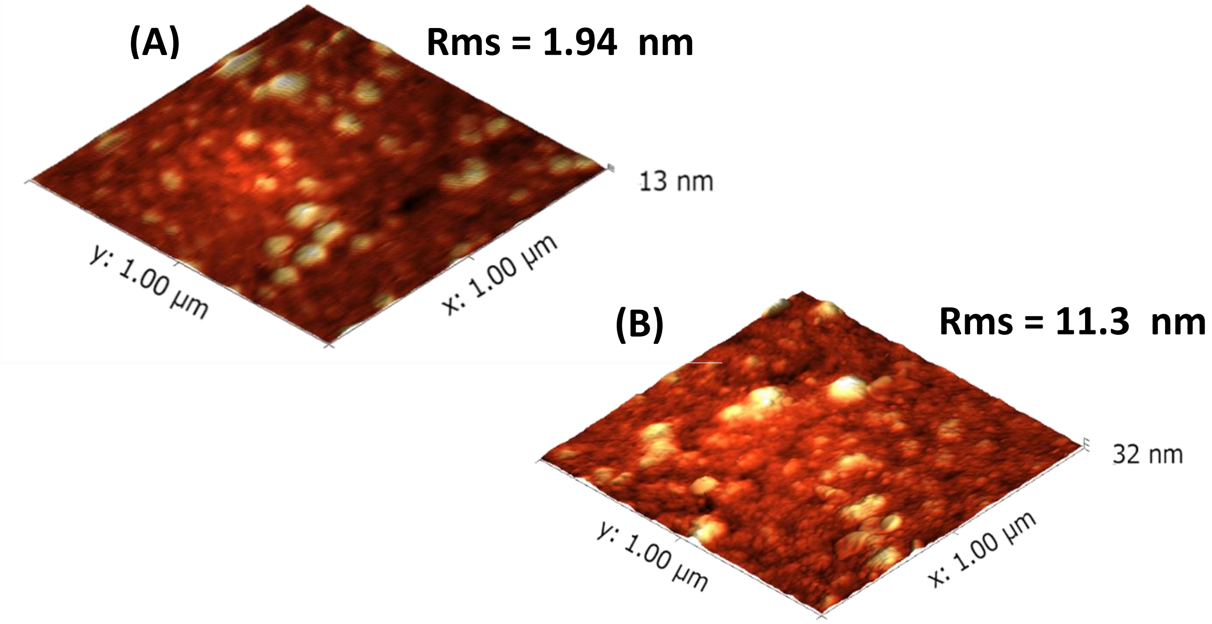

Figure S15: AFM micrographs and surface roughness values for SnTe thin films deposited by AA-CVD from 0.08 M toluene solutions of precursor **18** at 300 °C onto a glass substrate and at 400 °C onto a c-Si substrate.

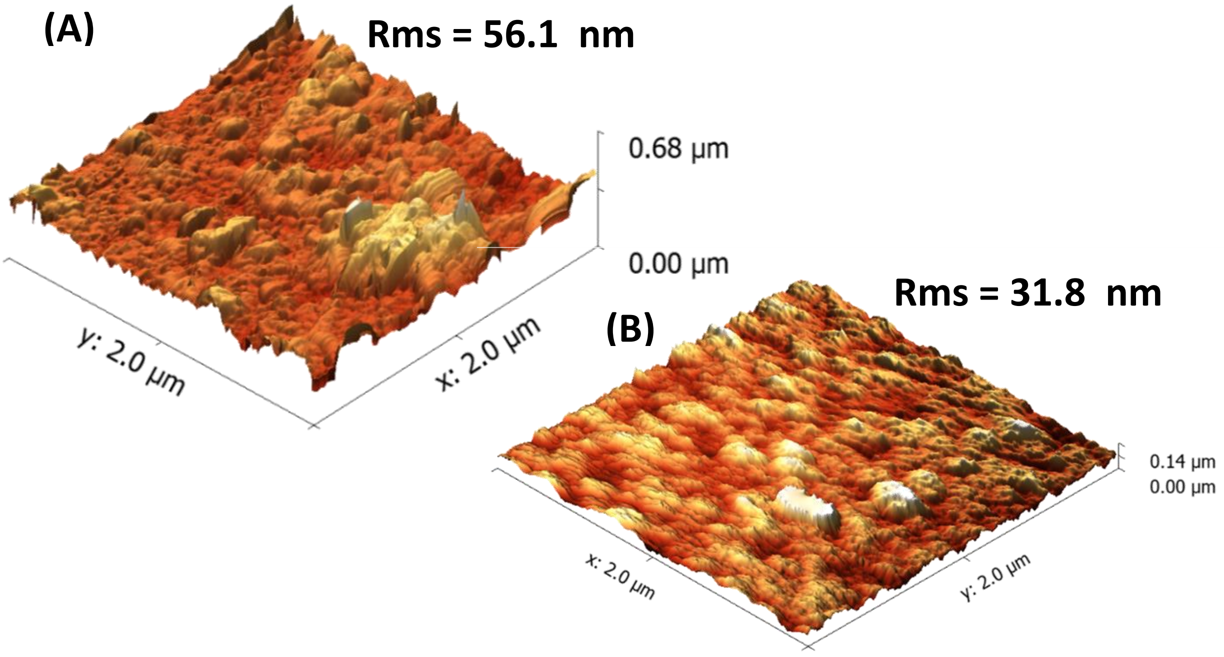

Figure S16: A diagram of the AA-CVD apparatus used in this study.

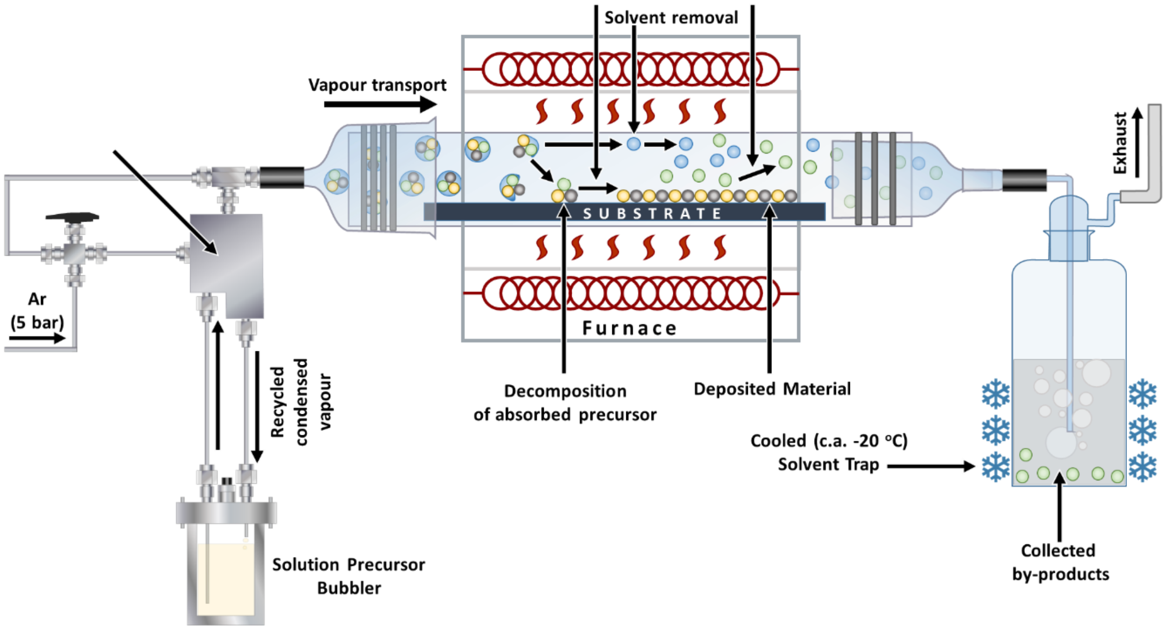

Table S5: Overview of Sn, SnS, SnSe and SnTe films deposited by AA-CVD from 0.08 M solutions of precursors **6**, **7**, **14**, **16**, and **18**.

Precursor	**Dep. Temp. (°C)**	**Substrates**	**Was a visible film deposited?**	**Detected Materials**	**Film Appearance**
6	**300**	Glass	**Yes**	**Sn** (Metallic)	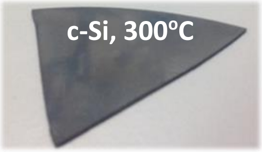 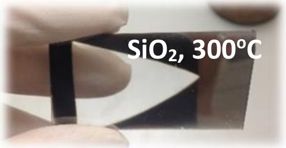
		c-Silicon	**Yes**		
	400	Glass	**Yes**		
		c-Silicon	**Yes**		
7	**300**	Glass	**Yes**		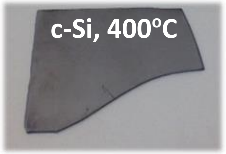 
		c-Silicon	**Yes**		
	400	Glass	**Yes**		
		c-Silicon	**Yes**		
14	**300**	Glass	**Non-continuous**	**α-SnS** (Non-adherent)	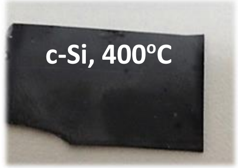 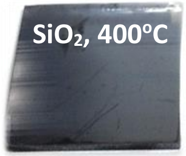
		c-Silicon	**Non-continuous**		
	400	Glass	**Non-continuous**		
		c-Silicon	**Yes**		
16	**300**	Glass	**No**	-	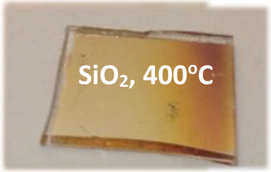
		c-Silicon	**No**	-	
	400	Glass	**Yes**	**α-SnSe**	
		c-Silicon	**Yes**		
18	**300**	Glass	**Non-continuous**	**SnTe** (Trace SnO)	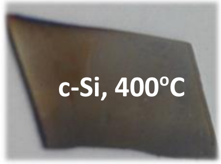 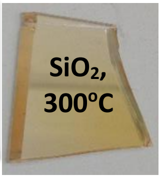 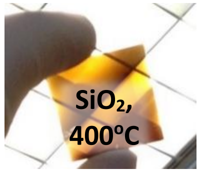
		c-Silicon	**Non-continuous**		
	400	Glass	**Yes**	**SnTe** (Trace SnO)	
		c-Silicon	**Yes**		

Table S6: Crystallographic data for compounds **7**,**8 10**-**1**

Compound	**7**	**8**	**10**	**11**	**12**
Chemical formula	$C_{30}H_{56}N_6Sn$	$C_{13}H_{30}N_4Sn$	$C_{54}H_{80}N_6Sn$	$2(C_{30}H_{56}N_6S_4Sn)$, $0.5(C_6H_{14})$	$C_{30}H_{56}N_6Se_4Sn\cdot C_4H_8O$
Formula Mass	619.49	361.10	931.93	1538.55	1007.44
Crystal system	Triclinic	Monoclinic	Monoclinic	Monoclinic	Monoclinic
a/Å	9.5182(2)	17.2010(3)	12.6165(2)	34.0180(6)	11.6920(2)
b/Å	13.6548(2)	8.66350(10)	31.8601(6)	10.6170(2)	18.7310(4)
c/Å	13.9233(2)	23.7650(3)	12.9872(2)	43.7820(8)	19.3700(3)
α/°	104.6350(10)	90	90	90	90
β/°	106.6654(9)	99.8642(9)	96.5982(12)	106.4110(10)	102.2130(10)
γ/°	101.5741(9)	90	90	90	90
Unit cell volume/Å^3	1602.89(5)	3489.13(9)	5185.79(15)	15168.5(5)	4146.08(13)
Temperature/K	150(2)	150(2)	150(2)	150(2)	150(2)
Crystal size /mm^3	0.15 x 0.13 x 0.13	0.13 x 0.10 x 0.08	0.25 x 0.20 x 0.18	0.2 × 0.2 × 0.2	0.18 x 0.15 x 0.10
Space group	$P\bar{1}$	*P21/a*	*P21/n*	*C2/c*	*C2/c*
Z	2	8	4	8	4
Radiation type	MoKα	MoKα	MoKα	MoKα	MoKα
2Θ range	1.613 to 27.490	3.593 to 27.473	3.006 to 28.308	7.19 to 55.122	3.258 to 27.508
Absorption coefficient, *μ*/mm^{-1}	0.824	1.457	0.532	0.923	4.161
No. of reflections measured	25814	51109	48761	109557	35347
No. of independent reflections	7327	7956	12533	17371	4753
R_{int}	0.0233	0.0694	0.0591	0.0986	0.0529
Final R_1 values ($I > 2\sigma(I)$)	0.0214	0.0315	0.0532	0.0451	0.0292
Final $wR(F^2)$ values ($I > 2\sigma(I)$)	0.0534	0.0669	0.1081	0.1248	0.0390
Final R_1 values (all data)	0.0235	0.0468	0.0880	0.0672	0.0663
Final $wR(F^2)$ values (all data)	0.0548	0.0735	0.1185	0.1399	0.0704
Goodness-of-fit on F^2	1.059	1.064	1.132	1.051	1.043
Largest diff. peak/hole / e Å^{-3}	0.438/-0.651	0.499/-0.894	0.534/-0.627	0.95/-0.87	1.042/-0.689
CCDC number	1814512	1814516	1814515	1814520	1814513

Table S7: Crystallographic data for compounds **11&13**, **15**-**18**

Compound	**11 & 13**	**15**	**16**	**17**	**18**
Chemical formula	$(C_{30}H_{56}N_6S_{5.31}Sn)\cdot 1.5(C_7H_8)$	$C_{36}H_{80}N_{12}Se_2Sn_2$	$C_{30}H_{56}N_6SeSn$	$C_{18}H_{40}N_6SnTe$	$C_{30}H_{56}N_6SnTe\cdot C_7H_8$
Formula Mass	1856.03	1076.42	698.45	586.85	839.23
Crystal system	Monoclinic	Monoclinic	Monoclinic	Monoclinic	Monoclinic
a/Å	10.4359(7)	13.94080(10)	12.2422(3)	14.6986(3)	12.2727(3)
b/Å	40.547(3)	23.6098(3)	26.8816(3)	9.2690(2)	27.0616(7)
c/Å	10.8210(8)	15.9826(2)	12.4038(6)	18.3539(4)	12.3569(3)
α/°	90	90	90	90	90
β/°	95.862(4)	109.3502(6)	103.1790(10)	97.4870(10)	103.8905(10)
γ/°	90	90	90	90	90
Unit cell volume/Å^3	4554.9(6)	4963.34(10)	3974.5(2)	2479.24(9)	3983.94(17)
Temperature/K	150(2)	150(2)	150.15	150(2)	150(2)
Crystal size /mm^3	0.13 x 0.10 x 0.08	0.25 x 0.20 x 0.130	0.2 × 0.2 × 0.15	0.20 x 0.15 x 0.13	0.20 x 0.17 x 0.08
Space group	*P21/a*	*C2/c*	*P21/a*	*P21/a*	*P21/a*
Z	2	4	4	4	4
Radiation type	MoKα	MoKα	MoKα	MoKα	MoKα
2Θ range	3.60 to 25.00	3.016 to 27.485	3.03 to 55.468	3.346 to 27.563	2.269 to 24.747
Absorption coefficient, μ/mm^{-1}	0.840	2.510	1.582	2.197	1.391
No. of reflections measured	36115	41171	43124	40910	43960
No. of independent reflections	7867	5661	8952	5675	6747
R_{int}	0.1419	0.0468	0.1157	0.0979	0.0583
Final R_1 values ($I > 2\sigma(I)$)	0.0926	0.0262	0.0552	0.0346	0.0360
Final $wR(F^2)$ values ($I > 2\sigma(I)$)	0.1742	0.0609	0.1568	0.0801	0.0859
Final R_1 values (all data)	0.1559	0.0292	0.0645	0.0479	0.0456
Final $wR(F^2)$ values (all data)	0.1965	0.0620	0.1658	0.0866	0.0908
Goodness-of-fit on F^2	1.146	1.146	1.099	1.066	1.254
Largest diff. peak/hole / e Å^{-3}	0.713/-0.848	0.763/-0.960	0.63/-1.07	0.755/-1.074	0.629/-0.679
CCDC number	1814514	1814517	1814518	1814521	1814519

Experimental details relating to the single-crystal X-ray crystallographic studies are summarised in Tables S6.
Crystallographic data were collected at 150 K on either a Nonius Kappa-CCD Diffractometer or an Oxford Diffraction Gemini Ultra Diffractometer, [λ(Cu$_{k\alpha}$) = 1.54184 Å] or [λ(Mo$_{k\alpha}$) = 0.71073 Å], and solved by direct methods and refined against all F^2 using SHELXL–97.[1]

Where possible non-hydrogen atoms are modelled as anisotropic and hydrogen atoms were constrained using a riding model. Absorption corrections, were appropriate, were performed using either analytical or semi-empirical methods. The data handling for complexes **7**, **8**, **12**, **15** and **18** require no special mention here.

In the asymmetric unit cell of **10** comprises of one molecule of the complex in which the Sn centre is disordered over two sites in 9:1 ratio. In additionally two i-Pr groups (C33-C35/C331A-C35A and C45-C47/C45A-C457) of the ligands are disordered over two positions in the ratio 65:35. The disorder was modelled anisotropically in order to assist convergence of the data.

The asymmetric unit cell of **11** comprises of two independent molecules of the Sn complex and 0.5 molecule of hexane of crystallisation per asymmetric unit; The hexane molecule is located on a twofold axis and is therefore disordered over two sites. Isotropic refinement with a 50% occupancy along with bond lengths and ADP restraints. However, this did not lend itself well to disorder modelling and hence, was treated using the solvent-mask algorithm in Olex 2.
50:50 disorder in the cyclohexyl rings attached to N22 and N12. The nitrogen to alpha carbon distances were restrained to being similar in these cases. The solvent was a disordered hexane moiety with half site-occupancy. However, this did not lend itself well to disorder modelling and hence, was treated using the solvent-mask algorithm in Olex 2.

The asymmetric unit cell of **11 & 14** comprises contains one molecule of Sn complex and 1.5 molecules of toluene of crystallisation. The Sn-complex coordinates a mixture of {S_6} ligand and {S_4} ligands which were the occupancy of which was modelled anisotopically using a free variable model (approx. 65:35 ratio). One solvent molecule is disordered over two sites in the ratio 3:1 and the other solvent molecule is disordered over an inversion centre and was refined with 50% occupation. All solvent molecule atoms were refined anisotopically with geometric constraints and ADP restraints.

In the case of complex **16** solvent masks have been used to remove random solvent peaks that could not be refined to produce a chemically sensible moiety. The residual electron density removed was 396.3 electrons over a cell volume of 986.0 cubic Angstroms.

The asymmetric unit in the structure of compound **17** was seen to comprise of one molecule of the Sn complex in which one of the iPr groups attached to the coordinated guanidinate ligand is disordered over two positions: The disorder was modelled anisotropically in a 40:60 occupancy ratio in order to assist convergence of the data.

References

1. G. M. Sheldrick, *Acta Crystallogr. A*, 2008, **64**, 112-122.